



Published in final edited form as:

J Dent Res. 2008 December ; 87(12): 1127–1132.

Damage Maps of Veneered Zirconia under Simulated Mastication

Jae-Won Kim, Joo-Hyung Kim, Malvin N. Janal¹, and Yu Zhang*

Department of Biomaterials and Biomimetics, New York University College of Dentistry, 345 East 24th Street, New York, NY 10010

¹Department of Psychiatry, New Jersey Medical School, Newark, New Jersey 07101-1709

Abstract

Zirconia based restorations often fracture from chipping and/or delamination of the porcelain veneers. We hypothesize that veneer chipping/delamination is a result of the propagation of near-contact induced partial cone cracks on the occlusal surface under mastication. Masticatory loading involves the opposing tooth sliding along the cuspal inner incline surface with an applied biting force. To test this hypothesis, flat porcelain veneered zirconia plates were cemented to dental composites and cyclically loaded (contact–slide–liftoff) at an inclination angle as a simplified model of zirconia based restorations under occlusion. In the light of in-situ observation of damage evolution in a transparent glass/zirconia/polycarbonate trilayer, postmortem damage evaluation of porcelain/zirconia/composite trilayers using a sectioning technique revealed that deep penetrating occlusal surface partial cone fracture is the predominant fracture mode of porcelain veneers. Clinical relevance is discussed.

Keywords

porcelain veneered zirconia structure; cyclic contact–slide fatigue; occlusal partial cone fracture; damage map; veneer fracture/chipping

INTRODUCTION

Ceramics are materials of choice for full coverage crowns and fixed partial dentures (FPDs) because of an increasing demand for aesthetics, biological acceptance, and chemical durability. Zirconia is the only ceramic material which meets the flexural strength requirements for FPDs of 4 or more units as recommended by the International Organization for Standardization (ISO 1999). Yet while strong, due to limited translucency, zirconia has been veneered with aesthetic porcelain to gain clinical acceptance. Clinical studies of veneered zirconia restorations indicate that while the zirconia cores are very fracture resistant, fracture/chipping of the porcelain veneer during mastication is a frequent problem (Raigrodski et al., 2006; Sailer et al., 2007a; Sailer et al., 2007b; Vult von Steyern et al., 2005).

*Corresponding author: yz21@nyu.edu.

Presented before the 37th General Session & Exhibition of the AADR April 2008, Dallas, Texas, USA

Occlusion is a complex phenomenon (Ulhaas et al., 2004). However, to first approximation, posterior tooth contact in a chewing cycle can be visualized as a sphere of several millimeters in diameter (Krejci et al., 1999) contacting the tip of a mesial-distal cusp ridge, sliding down toward central fossa, and then lifting off [Fig. 1(a)] (DeLong and Douglas, 1983; Kim et al., 2007b). Previously, by loading a transparent glass layer on polycarbonate system at an inclination angle (off-axis loading) in water, fracture mechanics models concerning damage evolution in single-layer glass-ceramics on compliant substrates have been established based on in-situ observations [Fig. 1(b)] (Kim et al., 2008; Zhang et al., 2008b). Near-contact induced partial cone cracks initiate at the occlusal surface and propagate to the ceramic-cement interface, while flexure-induced radial cracks originate from the cementation surface and propagate upward and sideward. Partial cone fracture dominates in thick layers ($d > 1$ mm), while radial fracture dominates in thin layers (Zhang et al., 2008a).

In this study, we extend the off-axis fatigue loading to study porcelain veneered zirconia structures cemented to dental composites [Fig. 1(c)]. Since the porcelain/zirconia/composite trilayer structure is an opaque system, damage sustained from the off-axis fatigue loading is examined using the sectioning technique (Mikosza and Lawn, 1971). Glass veneered zirconia structures are used as controls.

MATERIALS & METHODS

Material systems

30 fully sintered CAD/CAM zirconia plates ($\phi 15 \times 0.5$ mm, Lava™ Frame, 3M ESPE, St. Paul, MN) were veneered with overlay porcelain (Lava™ Ceram, 3M ESPE) by the manufacturer. The cementation surface of the zirconia core was roughened with 600-grit SiC abrasive paper and cemented (RelyX™ ARC, 3M ESPE) to a composite block ($\phi 15 \times 4$ mm, Z100™, 3M ESPE). The porcelain surface was polished to 1 μ m finish. The final dimensions of the veneered zirconia specimens were $\phi 15 \times 1.5$ mm. The composite blocks were incubated in water for 4 weeks before cementation to allow for hygroscopic expansion. After cementation, the bonded structures were aged in water for 10 days before fatigue testing.

As a control, 20 sintered CAD/CAM zirconia plates were “veneered” with soda-lime glass. The glass plates ($25 \times 25 \times 1$ mm, Daigger, Wheeling, IL) were polished on their side surfaces for in-situ viewing during testing. The top surfaces of the glass plates were abraded with 600-grit SiC to generate an adequate flaw density for cone crack initiation. The glass plates were joined to zirconia cores with a thin layer ($\sim 10 - 20$ μ m) of epoxy adhesive, which was allowed to cure for 48 hrs. The glass “veneered” zirconia structures were then epoxy bonded to the polycarbonate substrates (12.5 mm thick, AlN Plastics, Norfolk, VA). Because soda-lime glass and Y-TZP exhibit a large difference in coefficient of thermal expansion (CTE), this method avoids large residual thermal stresses to the system upon cooling. A thin layer of epoxy produces negligible stresses to the system during curing and does not deform substantially to cause significant flex of the glass veneer upon loading (Bhowmick et al., 2007).

Fatigue tests

Hertzian indentation fatigue tests were performed on veneered zirconia structures on compliant substrates with spherical tungsten carbide indenters of radius $r = 1.5$ mm in water using a mouth-motion simulator (Elf 3300, EnduraTEC Division of Bose, Minnetonka, MN). The specimen was mounted on an inclined block [$\theta = 30^\circ$, Fig. 1(c)]. Load was applied in the vertical direction, but the loading consisted of a contact–load–slide–liftoff sequence: the indenter contacting the specimen, loading to a maximum while sliding down the surface to create a wear facet ~ 0.5 mm in length, unloading and lifting off from the specimen surface. A loading and unloading rate of 1000 N/s was employed.

The current fatigue tests were designed to determine the type of damages and the number of cycles to failure n_F for a range of prescribed fatigue loads 160 N to 500 N. A minimum of three specimens were tested for each prescribed fatigue load. Failure of brittle layers on compliant substrates was defined when one of the occlusal surface crack systems reached the veneer/core interface or cementation internal surface radial cracks initiated. Damage maps were constructed for veneered zirconia on compliant substructures. For porcelain veneered zirconia systems, all specimens were subjected to post-mortem damage examination using combined optical microscopy (3D polarized specular reflection microscope, Edge R400, Micro Science Technologies, Marina Del Rey, CA) and a sectioning technique (Kim et al., 2007a). For glass veneered zirconia systems, all tests were recorded using a video camcorder (Canon XL1, Canon, Lake Success, NY) equipped with a microscope zoom system (Zhang et al., 2005). Analysis of variance (ANOVA) was used to compare test loads between groups, and to compare the number of cycles to failure as a function of veneering materials (porcelain or glass), while adjusting for differences in the loads employed. Cycles to failure were \log_{10} transformed before analysis. Statistical tests that yielded p-levels < 0.05 were considered significant.

RESULTS

Crack morphology

In off-axis fatigue loading of glass/zirconia/polycarbonate trilayers at $P = 300$ N [Fig. 2(a)], video frames captured from the side view revealed that a series of partial cone cracks (distorted classical cone cracks) formed in the first contact–load–slide–liftoff cycle. The trailing edges of the partial cones had an inclination angle $\alpha = 52 \pm 10^\circ$, which was much steeper than for classical cones in axial loading ($\alpha = 22 \pm 5^\circ$) (Kocer and Collins, 1998). Intrusion of water into the partial cone cracks was evident from the second load–slide cycle. The partial cones propagated steadily throughout the entire glass thickness, which differed from the previous reports of fatigue on glass/polycarbonate bilayers where partial cones surged abruptly to the glass polycarbonate interface once they approached the halfway point through the glass thickness (Kim et al., 2008). At $P = 500$ N [Fig. 2(b)], near-contact induced occlusal surface cracks reached glass/zirconia interface in the first load–slide cycle. Detailed frame to frame analysis of the video footage showed a series of partial cones formed at the trailing edges of the indenter upon loading. Further loading generated a median crack at the leading edge of the moving indenter. Finally, near the peak load, the median crack reached the glass/zirconia interface.

Analogous to the in-situ side view video sequences (Fig. 2), post-mortem sectional images revealed damage sustained in glass/zirconia/polycarbonate [Fig. 3(a)] and porcelain/zirconia/composite [Fig. 3(b)] trilayers following off-axis fatigue at $P = 350$ N for various loading cycles. A set of partial cones formed at the first contact–load–slide–liftoff cycle in both glass and porcelain veneers. However, it took only 5 cycles for the partial cones to penetrate through the entire porcelain veneer, whereas 7000 cycles were required for the partial cones to propagate through the glass “veneer”. The median cracks that appeared in high load fatigue of glass veneered zirconia [Fig. 2(b)] were not observed in the porcelain/zirconia/composite system under the load range tested.

Damage maps

Damage maps (load-cycles-type of failure) are reported for occlusal surface damage in porcelain/zirconia/composite (solid triangles) and glass/zirconia/polycarbonate (open and gray filled circles) trilayers subjected to off-axis fatigue loading [Fig. 4(a)]. Failure was predominately from the deep penetrating occlusal surface partial cone fracture; cementation radial fracture was not observed in the load range tested. Failure from occlusal surface median fracture was only observed in glass/zirconia/polycarbonate trilayers at high load $P = 500$ N. Median fracture was absent in porcelain/zirconia/composite trilayers for the load range investigated (i.e. 160 – 450 N). A previous study demonstrated that median cracks were more prevalent than cone cracks at high loads where the compressive stresses under the indenter became significant. For comparison, a damage map relating occlusal surface partial cone fracture in glass/polycarbonate bilayers under off-axis fatigue loading in a previous study is shown [Fig. 4(b)]. Inspection shows that fewer cycles (by over several orders of magnitude) were required to propagate occlusal surface partial cone cracks through the entire glass layer in glass/polycarbonate bilayers than the veneer layers (glass or porcelain) in veneered zirconia on compliant substrate trilayers.

Returning to the damage maps of veneered zirconia trilayers [Fig. 4(a)], ANOVA showed that significantly higher loads were used to test the glass/zirconia/polycarbonate [Mean (SD) = 372.5 N (85.0)] than the porcelain/zirconia/composite [Mean (SD) = 270.5 N (87.2)] samples [$F(1, 37) = 13.7, p = 0.001$]. Given this differences in loads, there was little difference between glass/zirconia/polycarbonate and porcelain/zirconia/composite samples in fatigue life, about 600 and 424 cycles, respectively [$F(1, 37) = 0.05, p = 0.82$]. However, when this analysis was adjusted for the load employed, analysis of covariance (ANCOVA) showed a significantly longer lifetime for glass/zirconia/polycarbonate than porcelain/zirconia/composite samples [$F(1, 36) = 153.8, p < 0.001$]. At a projected load of 322.8 N, glass/zirconia/polycarbonate samples would be expected to survive a mean of 3.87 logcycles (about 7400 cycles) while porcelain/zirconia/composite samples would be expected to survive only 1.475 logcycles (about 30 cycles). Thus, given comparable loads, glass/zirconia/polycarbonate specimens showed longer fatigue lifespan regarding occlusal partial cone fractures than porcelain/zirconia/composite specimens.

DISCUSSION

This study investigated the crack modes and fatigue life of veneered zirconia structures using a hard sphere on inclined ($\theta = 30^\circ$) porcelain/zirconia/composite trilayers, analogous to tooth contact during mastication. In the light of in-situ crack evolution in the model glass/zirconia/polycarbonate system, damage sustained in the porcelain/zirconia/composite system has been identified: contact–slide induced partial cone fractures initiated at the occlusal surface and propagated downward, ceasing at the porcelain/zirconia interface. These findings differ from earlier studies of veneered alumina and single-layer glass-ceramic systems where both contact induced occlusal surface cone fractures and flexure induced cementation surface radial fractures were evident (Rekow et al., 2007). Occlusal surface cone fractures can result in veneer fracture, chipping, and/or delamination, whereas cementation surface radial cracks can lead to catastrophic bulk fracture of ceramic restoration (Kelly et al., 1990). Our findings are consistent with clinical reports (Donovan, 2005; Oden et al., 1998; Raigrodski et al., 2006; Sailer et al., 2007a; Sjogren et al., 1999; Vult von Steyern et al., 2005).

In a veneered zirconia system, the stiff zirconia core provides stress shielding of the veneer layer and the underlying tooth structure (Lawn et al., 2007). The exceptionally high strength of the zirconia core prevents flexure induced cementation surface radial fracture. The relatively high modulus of the zirconia core (relative to porcelain) minimizes flexure of the porcelain veneer and propagation of partial cone cracks. In a single-layer glass-ceramic on composite system, the partial cones are initially driven by hydraulic pumping of water into the crack fissures and moisture-assist slow crack growth (SCG) (Kim et al., 2007b). However, when the cracks reach the mid thickness of the glass-ceramic layer, they begin to experience a flexural tensile stress field resulting from plate bending. This flexural tensile stress superimposes to the existing hydraulic pumping and SCG driving forces, resulting in partial cone cracks to surge abruptly to the ceramic/composite interface (Kim et al., 2008). With the support of a stiff zirconia core, flexure of the veneer layer is suppressed, resulting in a steady pace propagation of partial cones throughout the entire veneer layer.

The porcelain veneer and glass “veneer” show the same characteristics of damage modes and fracture behavior in response to contact–slide indentation, but differ in fatigue lifespan. The identical damage modes in porcelain and glass veneers are evident by the in-situ and postmortem damage assessment using optical microscopy. The same fracture behavior of porcelain and glass is supported by the similar slope of the number of cycles – fatigue load curves (damage maps) of the two materials, suggesting that the underlying mechanisms for crack propagation are identical in the two systems. The slope of the number of cycles – fatigue load curve is much shallower for glass/polycarbonate bilayers than veneer/zirconia/compliant trilayers, indicating the presence of additional driving forces—the flexure induced tensile stresses—in the glass/polycarbonate system.

The difference in fatigue lifespan of porcelain and glass veneers may be attributed to the differences in microstructure of the two materials, as well as the residual thermal stresses induced from mismatches in thermal conductivity and/or CTE of porcelain veneer and zirconia core. Soda-lime glass is an amorphous solid that lacks microstructural features,

such as pores and microcracks. Dental porcelains consist of crystals, feldspathic glass, grain boundaries, porosity, and microcracks. The residual stresses associated with the grain boundaries and sintering defects in porcelain can alter the crack propagation. In addition, although the CTE of Lava Ceram ($10 \times 10^{-6} \text{ K}^{-1}$) is closely matched with the Lava Frame ($10 \times 10^{-6} \text{ K}^{-1}$), at least in the temperature range studied (25 – 500°C, technical product profile, Lava™, 3M ESPS), residual thermal stresses still could be induced to the system through the veneering process. This is because (1) the CTE of veneering porcelains is nonlinear and varies with the temperature interval studied (Kingery et al., 1976); (2) dental porcelains typically experience phase changes as a result of thermal history (i.e. number of firings), which may affect the CTE of veneering materials (Isgro et al., 2005; Mackert et al., 1986); and (3) zirconia has a very low thermal conductivity ($2.0 - 2.2 \text{ Wm}^{-1}\text{k}^{-1}$) (Guess et al., 2008), which can result in large temperature gradients within the porcelain veneer during cooling, leading to residual thermal stresses. Our model glass veneered zirconia system, on the other hand, is joined with a thin epoxy adhesive layer at room temperature and thus free of residual thermal stresses (Bhowmick et al., 2007).

We acknowledge that the current flat veneered zirconia on composite system has its limitations to simulate other damage modes, particularly margin fractures, in anatomically shaped crowns and multi unit FPDs. Short (2 to 3 years) (Raigrodski et al., 2006; Vult von Steyern et al., 2005) to mid term (4 to 6 years) (Sailer et al., 2007a) clinical studies of veneered zirconia restorations revealed that fracture and chipping of the porcelain veneers were the predominant failure modes, only one incidence of a zirconia framework fracture, due to trauma was reported (Sailer et al., 2007a). Therefore, the current cyclic contact–slide fatigue of flat porcelain/zirconia/composite trilayers provides valuable insights to the fracture mechanisms of veneered zirconia restorations.

Acknowledgments

This investigation was supported in part by Research Grant 1R01 DE017925 (PI. Zhang) from the U.S. National Institute of Dental & Craniofacial Research, National Institutes of Health and Research Grant CMMI-0758530 (PI. Zhang) from the U.S. Division of Civil, Mechanical & Manufacturing Innovation, National Science Foundation.

References

- Bhowmick S, Meléndez-Martínez JJ, Zhang Y, Lawn BR. Design Maps for Failure of All-Ceramic Layer Structures in Concentrated Cyclic Loading. *Acta Materialia*. 2007; 55:2479–2488. [PubMed: 19562095]
- DeLong R, Douglas WH. Development of an artificial oral environment for the testing of dental restoratives: bi-axial force and movement control. *J Dent Res*. 1983; 62(1):32–6. [PubMed: 6571851]
- Donovan TE. Metal-Free Dentistry. *Journal of Esthetic and Restorative Dentistry*. 2005; 17(3):141–3. [PubMed: 15996382]
- Guess PC, Kulis A, Witkowski S, Wolkewitz M, Zhang Y, Strub JR. Shear bond strengths between different zirconia cores and veneering ceramics and their susceptibility to thermocycling. *Dent Mater*. 2008
- Isgro G, Kleverlaan CJ, Wang H, Feilzer AJ. The influence of multiple firing on thermal contraction of ceramic materials used for the fabrication of layered all-ceramic dental restorations. *Dent Mater*. 2005; 21(6):557–64. [PubMed: 15904699]
- Kelly JR, Giordano R, Pober R, Cima MJ. Fracture Surface Analysis of Dental Ceramics: Clinically Failed Restorations. *International Journal of Prosthodontics*. 1990; 3:430–40. [PubMed: 2088380]

- Kim B, Zhang Y, Pines M, Thompson VP. Fracture of porcelain-veneered structures in fatigue. *J Dent Res.* 2007a; 86(2):142–6. [PubMed: 17251513]
- Kim JH, Kim JW, Myoung SW, Pines M, Zhang Y. Damage maps for layered ceramics under simulated mastication. *J Dent Res.* 2008; 87(7):671–5. [PubMed: 18573989]
- Kim JW, Kim JH, Thompson VP, Zhang Y. Sliding contact fatigue damage in layered ceramic structures. *J Dent Res.* 2007b; 86(11):1046–50. [PubMed: 17959894]
- Kingery, WD.; Bowen, HK.; Uhlmann, DR. *Introduction to Ceramics. 2.* New York: John Wiley; 1976.
- Kocer C, Collins RE. The Angle of Hertzian Cone Cracks. *Journal of the American Ceramic Society.* 1998; 81(7):1736–42.
- Krejci I, Albert P, Lutz F. The influence of antagonist standardization on wear. *J Dent Res.* 1999; 78(2):713–9. [PubMed: 10029471]
- Lawn BR, Bhowmick S, Bush MB, Qasim T, Rekow ED, Zhang Y. Failure Modes in Ceramic-Based Layer Structures: A Basis for Materials Design of Dental Crowns. *Journal of the American Ceramic Society.* 2007; 90(6):1671–1683.
- Mackert JR Jr, Butts MB, Fairhurst CW. The effect of the leucite transformation on dental porcelain expansion. *Dent Mater.* 1986; 2(1):32–6. [PubMed: 3458629]
- Mikosza AG, Lawn BR. Section-and-Etch Study of Hertzian Fracture Mechanics. *Journal of Applied Physics.* 1971; 42(13):5540–45.
- Oden A, Andersson M, Krystek-Ondracek I, Magnusson D. Five-Year Clinical Evaluation of Procera AllCeram Crowns. *Journal of Prosthetic Dentistry.* 1998; 80(4):450–455. [PubMed: 9791792]
- Raigrodski AJ, Chiche GJ, Potiket N, Hochstedler JL, Mohamed SE, Billiot S, et al. The efficacy of posterior three-unit zirconium-oxide-based ceramic fixed partial dental prostheses: a prospective clinical pilot study. *J Prosthet Dent.* 2006; 96(4):237–44. [PubMed: 17052467]
- Rekow D, Zhang Y, Thompson V. Can material properties predict survival of all-ceramic posterior crowns? *Compend Contin Educ Dent.* 2007; 28(7):362–8. quiz 369, 386. [PubMed: 17687898]
- Sailer I, Feher A, Filser F, Gauckler LJ, Luthy H, Hammerle CH. Five-year clinical results of zirconia frameworks for posterior fixed partial dentures. *Int J Prosthodont.* 2007a; 20(4):383–8. [PubMed: 17695869]
- Sailer I, Pjetursson BE, Zwahlen M, Hämmerle CHF. A Systematic Review of the Survival and Complication Rates of All-Ceramic and Metal-Ceramic Reconstructions after an Observation Period of at Least 3 Years. Part II: Fixed Dental Prostheses. *Clin Oral Impl Res.* 2007b; 18(3):86–96.
- Sjogren G, Lantto R, Granberg A, Sundstrom BO, Tillberg A. Clinical Examination of Leucite-Reinforced Glass-Ceramic Crowns (Empress) in General Practice: A Retrospective Study. *Int J Prosthodont.* 1999; 12:122–8. [PubMed: 10371913]
- Ulhaas L, Kullmer O, Schrenk F, Henke W. A new 3-d approach to determine functional morphology of cercopithecoid molars. *Ann Anat.* 2004; 186(5–6):487–93. [PubMed: 15646282]
- Vult von Steyern P, Carlson P, Nilner K. All-ceramic fixed partial dentures designed according to the DC-Zirkon technique. A 2-year clinical study. *J Oral Rehabil.* 2005; 32(3):180–7. [PubMed: 15707428]
- Zhang Y, Song JK, Lawn BR. Deep-penetrating conical cracks in brittle layers from hydraulic cyclic contact. *J Biomed Mater Res B Appl Biomater.* 2005; 73(1):186–93. [PubMed: 15672403]
- Zhang Y, Kim JW, Bhowmick S, Thompson VP, Rekow ED. Competition of fracture mechanisms in monolithic dental ceramics: Flat model systems. *J Biomed Mater Res B Appl Biomater.* 2008a
- Zhang Y, Kim JW, Kim JH, Lawn BR. Fatigue damage in ceramic coatings from cyclic contact loading with a tangential component. *Journal of the American Ceramic Society.* 2008b; 91(1):198–202.

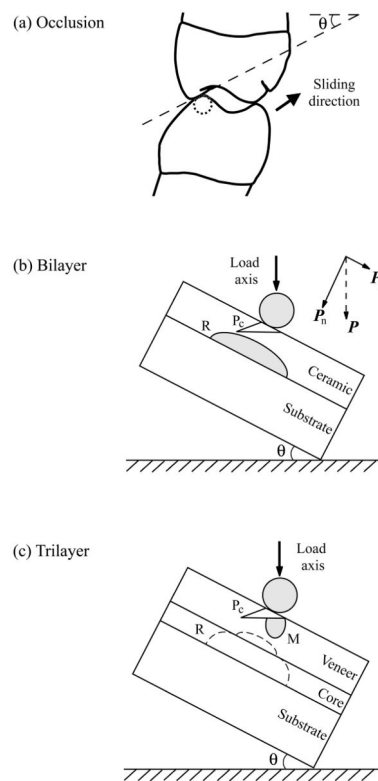


Fig. 1.

(a) Schematic of tooth eccentric occlusal position of right side first molar. Arrow indicates direction of sliding as teeth move to centric occlusion. Cuspal inclination slope and angulation (θ) are shown. (b) Experimental arrangement for indentation of brittle layer on compliant substrate (bilayer) with an inclination angle $\theta = 30^\circ$ (Off-axis loading). Showing two crack modes: occlusal surface partial cone cracks (P_c), and cementation surface radial cracks (R). Note the superposed tangential force component. (c) Experimental arrangement for indentation of veneered ceramic layer on compliant substrate (trilayer) with an inclination angle $\theta = 30^\circ$ (Off-axis loading). Showing three crack modes: occlusal surface partial cone cracks (P_c) and median cracks (M), and potential cementation surface radial cracks (R). Note cementation radial cracks are typically not observed in veneered zirconia systems in both clinical and in-vitro studies. However, in-situ laboratory testing show that once the cementation radial cracks form (at the bottom surface of the core layer), they propagate abruptly to the core/veneer interface and reinitiate at the bottom surface of the adjacent veneer layer, resulting catastrophic bulk fracture (Lawn et al., 2007).

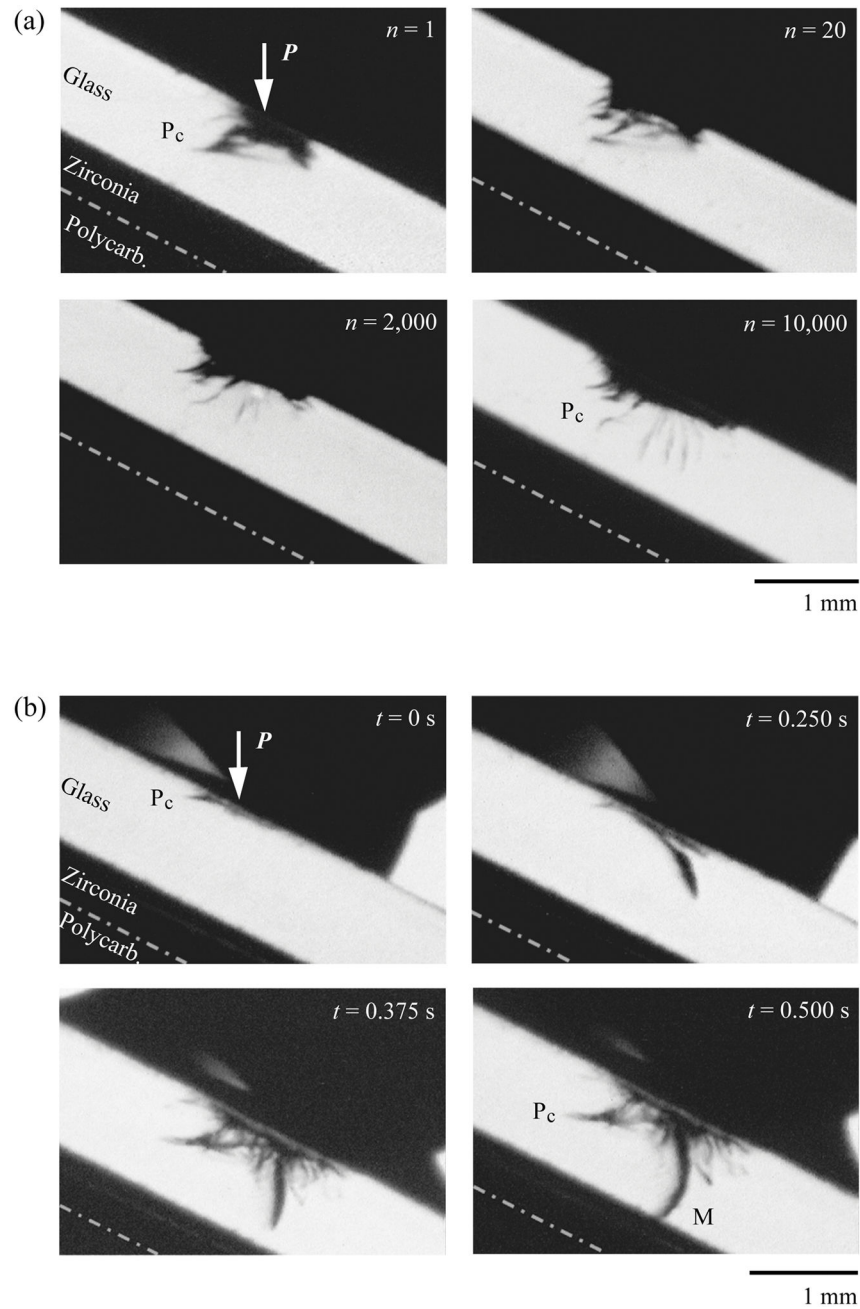


Fig. 2. Side view video sequence of evolving cracks in glass veneered zirconia plates on polycarbonate trilayers under off-axis loading at (a) $P = 300$ N following various numbers of cycle n and (b) $P = 500$ N in the first contact–slide cycle. Time, t , in seconds, s , for each video frames of (b) is estimated based on that a standard VCR captures 16 frames per second. Thus each video frame features a time interval of $1/16$ s. Indentation with tungsten carbide sphere of radius $r = 1.5$ mm, in water. Arrows (white) indicate the loading direction. Note in (a) partial cones (P_c) penetrate through the glass layer. In (b) partial cones (P_c) form at the first contact ($t = 0$ s, frame #1). Median cracks (M) form as the load increases ($t = 0.25$

s, frame #4). Although formed later than the partial cones, median cracks continue to dominate during the load–slide phase, eventually penetrate through the entire glass veneer at ($t = 0.5$ s, frame #8).

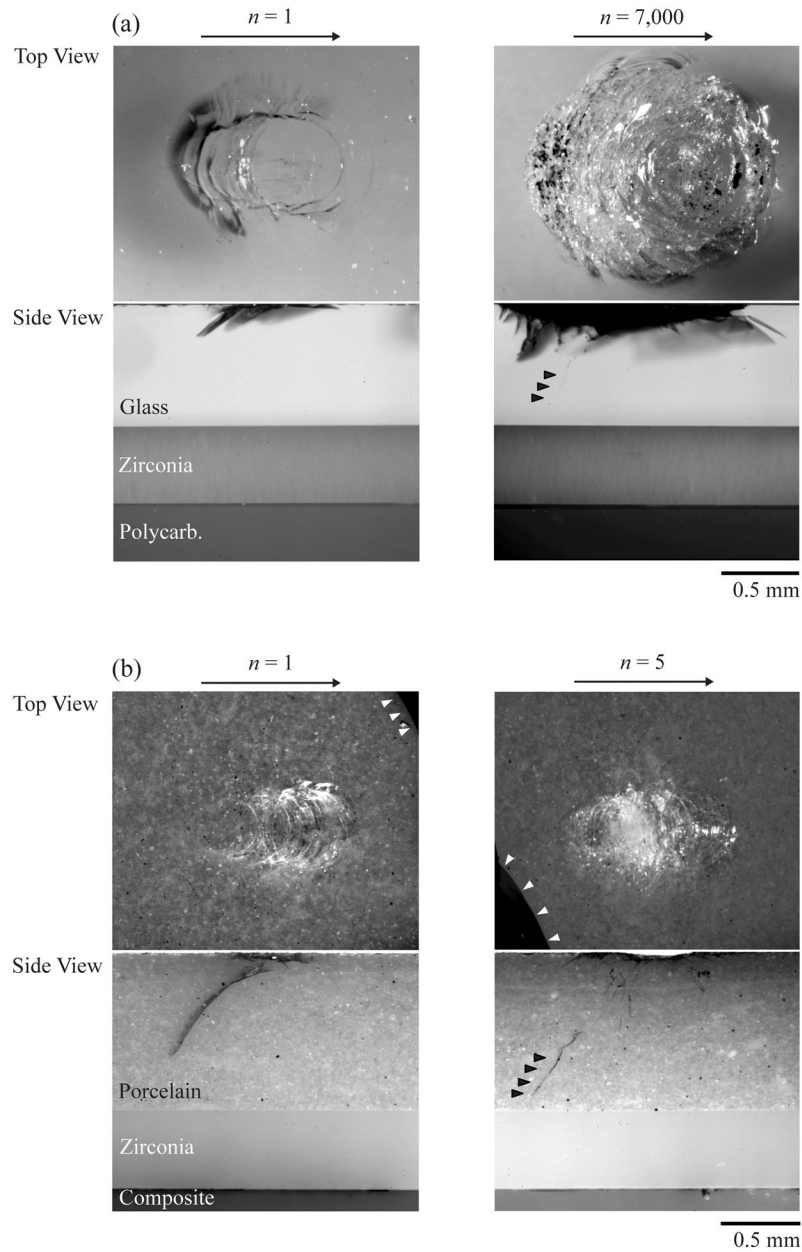


Fig. 3. Post-mortem optical micrographs showing top (occlusal) and side (section) views of (a) glass/zirconia/polycarbonate and (b) porcelain/zirconia/composite trilayers subjected to off-axis loading for single- and multi-cycles. Indentation with tungsten carbide sphere of radius $r = 1.5$ mm, $P = 350$ N, in water. Large arrows indicate the sliding direction for the off-axis test. Small black filled arrows highlight the trajectories of partial cone cracks. Small white arrows in (b) indicate the dark permanent markers used to index the contact region. Note in both cases, partial cones form in the first contact–slide cycle and continue to propagate through the veneer layers. However, the partial cone propagates much deeper in porcelain veneer after one contact-slide cycle and only take several cycles to propagate through the

porcelain veneer, while several thousands of cycles are required to drive partial cones to the glass/zirconia interface.

Author Manuscript

Author Manuscript

Author Manuscript

Author Manuscript

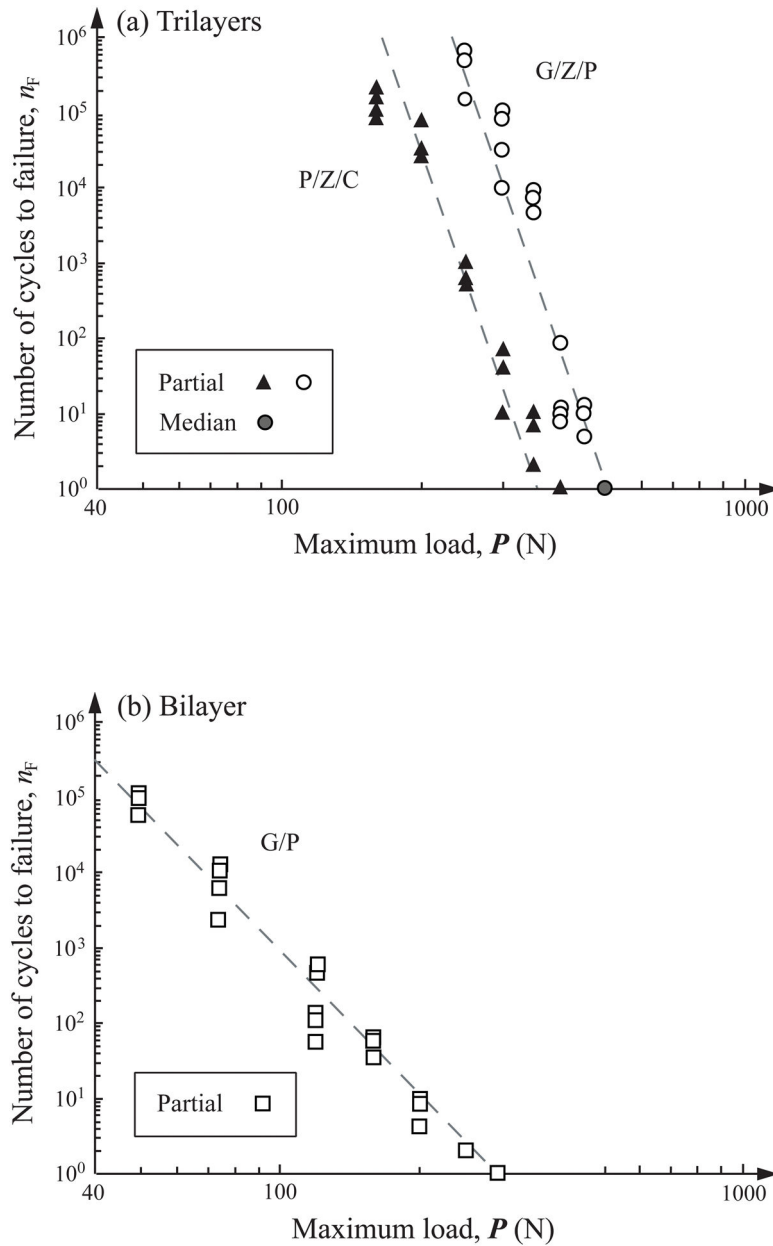


Fig. 4. Plot of number of cycles n_F to failure as a function of maximum load P for near-contact induced occlusal surface fractures in (a) porcelain/zirconia/composite (P/Z/C, solid triangles) and glass/zirconia/polycarbonate (G/Z/P, open and gray filled circles) trilayers and (b) glass/polycarbonate (G/P, open squares) bilayers following off-axis fatigue. In (a), the maximum fatigue loads P investigated are 160, 200, 250, 300, 350, 400 N for porcelain/zirconia/composite trilayers, and 250, 300, 350, 400, 450, 500 N for glass/zirconia/polycarbonate trilayers. Note in (a), median cracks (gray filled circle) are only observed at $P = 500$ N in glass/zirconia/polycarbonate trilayers. In (b), the maximum fatigue loads P used are 50, 75, 120, 160, 200, 250, 300 N for glass/polycarbonate bilayers. Indentation with

tungsten carbide sphere of radius $r = 1.5$ mm, in water. Failure occurs when occlusal cracks (either partial cone or median cracks) penetrate to veneer/zirconia or glass/polycarbonate interfaces at critical number of cycles n_F .

Author Manuscript

Author Manuscript

Author Manuscript

Author Manuscript